# Comparison of signal collection abilities of different classes of imaging spectrometers

R. Glenn Sellar[*a], Glenn D. Boreman[†b], Laurel E. Kirkland[‡c]
[a]Florida Space Institute, [b]University of Central Florida, [c]Lunar and Planetary Institute

## ABSTRACT

Although the *throughput* and *multiplex* advantages of Fourier transform spectrometry were established in the early 1950's (by Jacquinot[1,2,3] and Fellgett[4,5] respectively) confusion and debate[6] arise when these advantages are cited in reference to *imaging* spectrometry. In *non*-imaging spectrometry the terms *throughput* and *spectral bandwidth* clearly refer to the throughput of the entire field-of-view (FOV), and the spectral bandwidth of the entire FOV, but in *imaging spectrometry* these terms may refer to either the entire FOV or to a single element in the FOV. The continued development of new and fundamentally different types of imaging spectrometers also adds to the complexity of predictions of signal and comparisons of signal collection abilities. Imaging spectrometers used for remote sensing may be divided into classes according to how they relate the object space coordinates of cross-track position, along-track position, and wavelength (or wavenumber) to the image space coordinates of column number, row number, and exposure number for the detector array. This transformation must be taken into account when predicting the signal or comparing the signal collection abilities of different classes of imaging spectrometer. The invariance of radiance in an imaging system allows the calculation of signal to be performed at any space in the system, from the object space to the final image space. Our calculations of signal - performed at several different spaces in several different classes of imaging spectrometer - show an interesting result: regardless of the plane in which the calculation is performed, interferometric (Fourier transform) spectrometers have a dramatic advantage in signal, but the *term* in the signal equation from which the advantage results depends upon the space in which the calculation is performed. In image space, the advantage results from the spectral term in the signal equation, suggesting that this could be referred to as the multiplex (Fellgett) advantage. In an intermediate image plane the advantage results from a difference in a spatial term, while for the exit pupil plane it results from the angular term, both of which suggest the throughput (Jacquinot) advantage. When the calculation is performed in object coordinates the advantage results from differences in the temporal term.

Keywords: Fourier transform spectrometry, imaging spectrometry, remote sensing, throughput, etendue, signal-to-noise ratio

## 1. CLASSES OF IMAGING SPECTROMETERS

By definition, imaging spectrometers are designed to measure the flux collected from an object as a function of two spatial and one spectral dimensions. Most imaging spectrometers employ two-dimensional detector arrays, which collect flux as a function of column number, row number, and exposure number. In order to be useful, this raw data must be transformed from the image coordinate system of column, row, and exposure into the object coordinate system of cross-track position, along-track position, and wavelength (or wavenumber.)

Imaging spectrometers used for remote sensing may be divided into classes based on two aspects: the method by which they obtain spatial information, and the method by which they obtain spectral information. Methods of acquiring spatial information include whiskbroom, pushbroom, staring, and a new class we refer to as *windowing*. A whiskbroom-scanning instrument employs a 'zero-dimensional' FOV which scans the object in both the along-track and cross-track directions, while a pushbroom-scanning instrument scans a one-dimensional FOV in the along-track direction only. A staring instrument employs a two-dimensional FOV which remains fixed on the object. We use the term *windowing* to

[*] gsellar@mail.ucf.edu; phone 1 407 658-5597; fax 1 407 658-5595; Florida Space Institute, 12424 Research Parkway, Suite 400, Orlando, FL 32826;
[†] CREOL/School of Optics, University of Central Florida, Orlando, FL 32816-2700;
[‡] kirkland@lpi.usra.edu; Lunar and Planetary Institute, 3600 Bay Area Blvd., Houston, TX 77058-1113

describe the relatively new class of instruments that employ a two-dimensional FOV which moves across the object in the along-track direction.

Methods of acquiring spectral information include the familiar filtering, dispersive, and interferometric techniques. Dispersive instruments may use either a prism or a grating. By interferometric we refer to Fourier-transform spectrometers (FTS) employing two-beam interferometers such as the Michelson, Mach-Zender, or Sagnac. Multiple-beam interferometers such as the Fabry-Perot have signal collection abilities more similar to filtering instruments than to FTS.

This classification scheme, with examples of commonly used terms for each class, is illustrated in Table 1.

Table 1: Classification of Imaging Spectrometers

| | **Along-track Scanning** | | |
|---|---|---|---|
| **Spectral** | Pushbroom  | Windowing 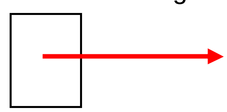 | Staring 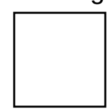 |
| Filtering | | Filter-array<br>Wedge filter<br>Linear variable filter | Band-sequential<br>Filter wheel<br>Tunable filter |
| Dispersive | Grating or prism | ? | Tomographic |
| Interferometric | Static FTS<br>(Sagnac) | Static FTS<br>(Mach-Zender, Sagnac) | Traditional FTS<br>(Michelson) |

## 2. BASIS FOR COMPARISON

A useful comparison of instruments must be based on identical performance requirements and identical constraints for each instrument. We define the performance requirements as the spatial sampling intervals (ground sample distances) across-track and along-track, the number of spatial samples across-track and along-track, the spectral range, and the number of spectral samples. A specification of spectral resolution in constant wavelength intervals would favor dispersive and filter instruments, while a specification of constant wavenumber intervals would favor interferometric instruments, so we specify only the spectral range and *number of spectral samples*, which is neutral. This set of requirements common to each instrument is summarized in Table 2, along with typical units.

Table 2: Common set of requirements

| | **Range** | **Sample extent** | **Number of samples** |
|---|---|---|---|
| **Cross-track** | $X$ [m] | $\Delta x$ [m] | $N_x$ |
| **Along-track** | $Y$ [m] | $\Delta y$ [m] | $N_y$ |
| **Spectral** | $\Lambda$ [μm] | $\Delta\lambda$ [μm] | $N_\lambda$ |
| **Temporal** | $\tau$ [s] | $\tau$ [s] | *1* |

The common set of constraints are: observation of the same object defined by its spectral radiance, observation from the same range, the same total time available to complete the acquisition task, use of identical detector arrays, and the same mass, which we constrain roughly by using the same size entrance aperture for each instrument. These constraints are summarized in Table 3.

Table 3: Common set of constraints

| | |
|---|---|
| Object Spectral Radiance | $L_\lambda$ [photons $s^{-1}$ $m^{-2}$ $sr^{-1}$ $\mu m^{-1}$] |
| Detector Array | Number of columns: $N_i$<br>Number of rows: $N_j$ |
| Mass | Entrance aperture determines $\Omega$ [sr] |

Note that the spectral units could be in either wavelength [µm] or wavenumbers [$cm^{-1}$] as long as both the spectral radiance and the spectral extent are in the same units. The number of exposures read from the array $N_k$ is not constrained.

## 3. SIGNAL CALCULATIONS

The signal is given by the following equation:

$$S = L_\lambda \eta (\Delta x)(\Delta y)\Omega(\Delta\lambda)(\Delta\tau)$$

where $S$ represents the signal in photons, $L_\lambda$ the spectral radiance of the object in photons $s^{-1}$ $m^{-2}$ $sr^{-1}$ $\mu m^{-1}$, $\eta$ the efficiency (dimensionless), $\Delta x$ the spatial extent in the cross-track direction in meters, $\Delta y$ the spatial extent in the along-track direction in meters, $\Omega$ the solid angle in steradians, $\Delta\lambda$ the spectral extent in microns, and $\Delta\tau$ the temporal extent in seconds.

Since throughput (the product of area and solid angle) is the same at any plane in a purely imaging system, if we ignore losses then *radiance* is also invariant through an imaging system. Thus one may use the same radiance when calculating the signal at any space in the system, including for the example the object space, the final image space, or even an intermediate image plane or a pupil plane.

### 3.1 Calculation in object space

When we perform the calculation in object space: $\Delta x$ is the spatial extent of an object *voxel* (sample element) in the cross-track direction, $\Delta y$ is the spatial extent of a voxel in the along-track direction, $\Omega$ is the solid angle subtended by the entrance aperture of the instrument as viewed from the object, $\Delta\lambda$ is the spectral extent of a voxel, and $\Delta\tau$ is the temporal extent during which flux is collected from that particular voxel. We immediately note that when the calculation is performed in object space the parameters $L_\lambda$ , $\Delta x$ , $\Delta y$ , $\Omega$ , and $\Delta\lambda$ are all determined by the common set of requirements and constraints and thus are by definition identical for all classes of imaging spectrometer. Only the efficiency $\eta$, and the temporal extent $\Delta\tau$ vary with the class of instrument. The efficiency term includes transmission and reflection losses, diffraction efficiency, and fringe modulation, as appropriate to each class of instrument. We arbitrarily - but reasonably - assign the following values for $\eta$:

Table 4: Determination of η

| | |
|---|---|
| Dispersive: | η = 1 (anti-reflection coated prism) |
| Filter: | η = 0.25 (average filter transmittance) |
| Interferometric: | η = 0.25 (modulation factor) |

Determination of the temporal extent $\Delta\tau$ is facilitated by drawing a diagram of the transmittance of each instrument in object space, as shown in Figure 1. For all of the instruments considered here, the transmittance does not vary with cross-track position *x*, so the transmittance functions are displayed as a function of along-track position *y* and wavelength $\lambda$. The arrows indicate how the transmittance function changes with time.

| *Spectral Class*<br>*Scan Class* | *Transmittance vs. y and λ* | $\Delta\tau$ |
|---|---|---|
| Filtering<br>Staring | λ 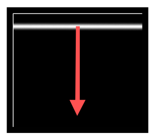 y | $\frac{\tau}{N_\lambda}$ |
| Dispersive<br>Pushbroom | λ  y | $\frac{\tau}{N_y}$ |
| Interferometric<br>Staring | λ 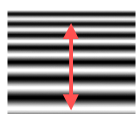 y | $\frac{\tau}{2}$ |
| Filtering<br>Windowing | λ 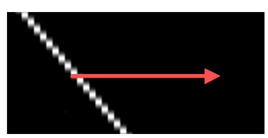 y | $\frac{\tau}{N_\lambda}\left(\frac{N_j}{N_y + N_j}\right)$ |
| Interferometric<br>Windowing | λ 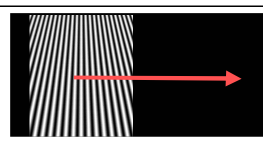 y | $\frac{\tau}{2}\left(\frac{N_j}{N_y + N_j}\right)$ |
| Panchromatic<br>Staring | λ 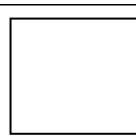 y | $\tau$ |

Figure 1: Determination of temporal extent $\Delta\tau$ for an object voxel

The panchromatic staring class, while obviously not an imaging spectrometer, is included in Figure 1 for purposes of comparison. Having determined all the factors in the signal equation in terms of the requirements and constraints, we can now compare the signal collection abilities of the different classes of imaging spectrometer. Table 5 shows the relative signal expected for each class. The signals have been normalized to that expected for a panchromatic imager by dividing out the parameters that are the same for all classes: $L_\lambda$ , $\Delta x$ , $\Delta y$ , $\Omega$ , and $\Delta\lambda$. A numerical example is also shown in Table 5 for a typical case with the number of samples along-track $N_y = 1000$, number of spectral samples $N_\lambda = 100$, and number of rows in the detector array $N_j = 1000$. The signals in this last column are normalized relative to the signal for the *dispersive pushbroom* class.

Table 5: Relative signal for an object voxel

| *Spectral Class*<br>*Scan Class* | *Relative Signal Factor*<br>$(\eta)(\Delta\tau)$ | *Relative Signal for example:* $N_y$=1000, $N_\lambda$=100, $N_j$=1000 |
|---|---|---|
| Filtering<br>Staring | $\left(\frac{1}{4}\right)\left(\frac{1}{N_\lambda}\right)$ | 2.50 |
| Dispersive<br>Pushbroom | $(1)\left(\frac{1}{N_j}\right)$ | 1.00 |
| Interferometric<br>Staring | $\left(\frac{1}{4}\right)\left(\frac{1}{2}\right)$ | 125.00 |
| Filtering<br>Windowing | $\left(\frac{1}{4}\right)\left(\frac{1}{N_\lambda}\frac{N_j}{N_y+N_j}\right)$ | 1.25 |
| Interferometric<br>Windowing | $\left(\frac{1}{4}\right)\left(\frac{1}{2}\frac{N_j}{N_y+N_j}\right)$ | 62.50 |
| Panchromatic<br>Staring | 1 | 1000.00 |

Here the most influential factor in determining the relative signal collected from each object voxel is clearly the *temporal* ($\Delta\tau$) factor. This may be surprising, since a throughput (Jacquinot) advantage would be expected to appear in the area·solid angle product ($\Delta x\Delta y\Omega$), and a multiplex (Fellgett) advantage would be expected to appear in the spectral ($\Delta\lambda$) factor. For an imaging spectrometer, when we consider the signal from a single object voxel, both the throughput and the spectral bandwidth terms are the same for every class of instrument. Fourier transform (interferometric) instruments do have a dramatic advantage in signal, but when the calculation is performed for individual object voxels this advantage results from the *temporal* term in the signal equation. When referring to imaging spectrometers, the term from which the signal advantage derives depends upon whether the signal is calculated for the entire FOV or for a single element, and also upon the space in which the calculation is performed. In order to avoid confusion it may be preferable to use a more general term for the advantage possessed by imaging FTS. Perhaps "*signal* advantage" would be a less confusing term.

### 3.2 Calculation in image space

The preceding analysis predicts the signal obtained from each object voxel, which is the signal of most relevance to the user of the data. But we may also perform the signal calculation in image space, thereby obtaining the signal in each element of the raw data before the raw data is transformed into the object coordinate system. If we perform the signal calculation in image space, the terms in the equation are defined as follows: $\Delta x$ and $\Delta y$ are the spatial extents of a pixel in the detector array, $\Omega$ is the solid angle subtended by the exit pupil of the optics as viewed from the detector array, $\Delta\lambda$ is the spectral extent of the flux allowed to reach the pixel, $\Delta\tau$ is the integration time for each exposure of the detector array. We immediately note that when the calculation is performed in image space the parameters $L_\lambda$, $\Delta x$, $\Delta y$, and $\Omega$ are all determined by the common set of requirements and constraints and thus are by definition identical for all classes of imaging spectrometer. In image space only the efficiency η, the spectral extent $\Delta\lambda$, and the temporal extent $\Delta\tau$ vary with the class of instrument. Also note that although we have constrained the *total* acquisition time $\tau$ to be the same for each instrument, the number of exposures $N_k$ and resultant individual exposure times $\Delta\tau$ are not constrained. Different classes of instrument acquire a different number of exposures (i.e. operate at different frame rates) in order to obtain the same number of processed elements *after* transformation into object space.

In a filtering spectrometer the filter restricts the spectral extent to bandwidth for any individual exposure to that of a single filter. Dispersive instruments spread the spectral range across the rows of the array, so a pixel on any row receives only a small fraction of the spectral range. Two-beam interferometers reject an average of one-half of the spectral range. The spectral extent $\Delta\lambda$, number of exposures $N_k$, and temporal extent $\Delta\tau$ in image space for each class of instrument are shown in Table 6.

Table 6: Spectral extent $\Delta\lambda$ for a raw data element, number of exposures $N_k$, and temporal extent $\Delta\tau$ for a raw data element

| *Spectral Class*<br>*Scan Class* | $\Delta\lambda$ | $N_k$ | $\Delta\tau$ |
|---|---|---|---|
| Filtering<br>Staring | $\frac{\Lambda}{N_\lambda}$ | $N_\lambda$ | $\frac{\tau}{N_\lambda}$ |
| Dispersive<br>Pushbroom | $\frac{\Lambda}{N_j}$ | $N_y$ | $\frac{\tau}{N_y}$ |
| Interferometric<br>Staring | $\frac{\Lambda}{2}$ | $2N_\lambda$ | $\frac{\tau}{2N_\lambda}$ |
| Filtering<br>Windowing | $\frac{\Lambda}{N_\lambda}$ | $N_y + N_j$ | $\frac{\tau}{N_y + N_j}$ |
| Interferometric<br>Windowing | $\frac{\Lambda}{2}$ | $N_y + N_j$ | $\frac{\tau}{N_y + N_j}$ |
| Panchromatic<br>Staring | $\Lambda$ | 1 | $\tau$ |

Having determined all the factors in the signal equation in image space, we can now predict the signal expected in each raw data element for each of the different classes of imaging spectrometer. Table 7 shows the relative signal expected for each class. The signals have been normalized to that expected for a panchromatic imager by dividing out the parameters that are the same for all classes: $L_\lambda$ , $\Delta x$ , $\Delta y$ , and $\Omega$. A numerical example is also shown in Table 7 for a typical case with the number of samples along-track $N_y$ = 1000, number of spectral samples $N_\lambda$ = 100, and number of rows in the detector array $N_j$ = 1000. The signals in this last column are normalized relative to the signal for the *dispersive pushbroom* class.

It is notable that the relative signal per element in image space is not the same as the relative signal per element in object space. This, however, is not surprising when we consider that while the number of object voxels is given by the product of the requirements $N_x N_y N_\lambda$ and is thus the same for each instrument, the number of *raw* data elements, given by the product $N_i N_j N_k$ , is *not* the same for each instrument. In any case, the signal of most relevance to the user of the data is the signal from each object voxel, rather than the signal in each raw data element. The calculation in image space is included here to demonstrate one interesting point: in image space the factor that most influences the relative signal in each raw data element is the *spectral* factor, which suggests the *multiplex (Fellgett) advantage*.

Table 7: Relative signal for a raw data element (image space)

| *Spectral Class*<br>*Scan Class* | *Relative Signal Factor*<br>$(\eta)(\Delta\lambda)(\Delta\tau)$ | *Relative Signal for example:* $N_y$=1000, $N_\lambda$=100, $N_j$=1000 |
|---|---|---|
| Filtering<br>Staring | $\left(\frac{1}{4}\right)\left(\frac{1}{N_\lambda}\right)\left(\frac{1}{N_\lambda}\right)$ | 25.00 |
| Dispersive<br>Pushbroom | $(1)\left(\frac{1}{N_j}\right)\left(\frac{1}{N_y}\right)$ | 1.00 |
| Interferometric<br>Staring | $\left(\frac{1}{4}\right)\left(\frac{1}{2}\right)\left(\frac{1}{2N_\lambda}\right)$ | 625.00 |
| Filtering<br>Windowing | $\left(\frac{1}{4}\right)\left(\frac{1}{N_\lambda}\right)\left(\frac{1}{N_y+N_j}\right)$ | 1.25 |
| Interferometric<br>Windowing | $\left(\frac{1}{4}\right)\left(\frac{1}{2}\right)\left(\frac{1}{N_y+N_j}\right)$ | 62.50 |
| Panchromatic<br>Staring | 1 | 1000000.00 |

### 3.3 Calculation in other spaces

In the intermediate planes in the instrument, such as an intermediate image plane or a pupil plane, the signal is not divided into elements. In a dispersive instrument, at the intermediate image plane the slit will determine the area factor ($\Delta x \Delta y$), while at the exit pupil plane the slit will determine the solid angle factor $\Omega$. Thus if we perform the analysis at either of these two planes and do not divide the flux into elements, then the advantage of interferometric instruments will appear as a throughput (Jacquinot) advantage.

## 4. CONCLUSIONS

From these analyses, we draw the following conclusions:

(1) Interferometric (or FTS) imaging spectrometers have a dramatic advantage in signal collection ability, approximately two orders of magnitude for typical specifications.

(2) The term in the signal equation from which the signal advantage results depends upon the space in which the calculation is performed.

(3) In image space the advantage results from the spectral term, suggesting the multiplex (Fellgett) advantage.

(4) In an intermediate plane, if the flux is not divided into elements, the advantage results from the area term or the solid angle term, suggesting the throughput (Jacquinot) advantage.

(5) In object space **-** which is the frame of most relevance to the user of the data **-** the advantage results from the temporal term.

Thus, in the context of *imaging* spectrometers, the terms throughput or Jacquinot advantage and multiplex or Fellgett advantage may lead to confusion. Fourier-transform imaging spectrometers, however, clearly do possess a dramatic advantage in signal collection ability. We recommend "*signal advantage*" as a more useful term for this property.

## ACKNOWLEDGEMENTS

This research was funded by NASA under grant number NAG5-10730.

## REFERENCES

[1] P. Jacquinot and C. Dufour, "Condition optique d'emploi des cellules photo-électriques dans les spectrographes et les interféremetrès, *Journal Recherche du Centre National Recherche Scientifique Laboratorie Bellevue*, **6**, pp. 91-103, Paris, 1948.
[2] P. Jacquinot, "The Etendue Advantage", *XVII me Congrs du GAMS*, Paris, 1954.
[3] P. Jacquinot, *J. Phys. Radium*, **19**, p. 223, 1958.
[4] P. B. Fellgett, *The Multiplex Advantage* Ph.D. Thesis, University of Cambridge, Cambridge, U. K., 1951.
[5] P. B. Fellgett, *J. Opt. Soc. Amer.*, **42**, p. 872, 1952.
[6] L. W. Schumann and T. S. Lomheim, "Infrared hyperspectral imaging Fourier transform and dispersive spectrometers: comparison of signal-to-noise-based performance," *Proc. SPIE*, **4480**, pp. 1-14, 2001.